

# Artistic Vision: Painterly Rendering Using Computer Vision Techniques

Bruce Gooch  
University of Utah

Greg Coombe  
University of North Carolina at Chapel Hill

Peter Shirley  
University of Utah

## Abstract

We present a method that takes a raster image as input and produces a painting-like image composed of strokes rather than pixels. Our method works by first segmenting the image into features, finding the approximate medial axes of these features, and using the medial axes to guide brush stroke creation. System parameters may be interactively manipulated by a user to effect image segmentation, brush stroke characteristics, stroke size, and stroke frequency. This process creates images reminiscent of those contemporary representational painters whose work has an abstract or sketchy quality. Our software is available at <http://www.cs.utah.edu/npr/ArtisticVision>.

**CR Categories:** I.3.7 [Computing Methodologies]: Computer Graphics—2D Graphics

**Keywords:** image moments, image processing, medial axis, non-photorealistic rendering, painting

## 1 Introduction

The art of painting relies on representation and abstraction. In representational painting, the abstraction occurs when the detail of real images is approximated with limited spatial resolution (brush strokes) and limited chromatic resolution (palette). Economy is a quality of many paintings, and refers to the use of only those brush strokes and colors needed to convey the essence of a scene. This notion of economy has been elusive for computer-painting algorithms. We explore an automated painting algorithm that attempts to achieve economy, particularly in its use of brush strokes.

There are two tasks involved in the creation of a digital painting. First is the creation of brush stroke positions, the second is the rendering of brush strokes. If the brush stroke positions are manually created by a user, then this is a classic paint program. If the brush stroke positions are computed algorithmically, then this is an automatic painting system. In either case, once the brush stroke geometry is known, the brush strokes must then be rendered, usually simulating the physical nature of paint and canvas [4, 17, 24].

We review digital painting strategies in Section 2 and give an overview of our algorithm in Section 3. The conversion from a single segment of an image to a set of planned brush strokes, which is the core of our contribution, is covered in Sections 4–8. We discuss possible extensions to our method in Section 9.

## 2 Background

Two basic approaches to digital painting are used in computer graphics. The first simulates the characteristics of an artistic medium such as paint on canvas. The second attempts to automatically create paintings by simulating the artistic process. These approaches can be combined because they deal with different aspects, one low-level and one high-level, of painting.

Work intended to simulate artistic media can be further divided into those which simulate the physics a particular medium, and those which just simulate the look. Strassmann [24] simulated the



Figure 1: A landscape painting of Hovenweep National Monument. This painting was automatically created using the system described in this paper. The input was a scanned vacation photograph.

look of traditional sumi-e painting with polylines and a raster algorithm. Pham [17] augmented this algorithm using B-splines and offset curves instead of polylines to achieve smoother brush paths. Williams [27] provides a method of merging painting and sculpting by using the raster image as a height field.

Smith [22] points out that by using a scale-invariant primitive for a brush stroke, multi-resolution paintings can be made. Berman et al. [1] showed that multi-resolution painting methods are efficient in both speed and storage. Perlin and Velho [16] used multi-resolution procedural textures to create realistic detail at any scale.

Several authors have simulated the interaction of paper/canvas and a drawing/painting instrument. Cockshott [4] simulated the substrate, diffusion, and gravity in a physically-based paint system. Curtis et al. [6] modeled fluid flow, absorption, and particle distribution to simulate watercolor. Sousa and Buchanan [23] simulated pencil drawing by modeling the physics and interaction of pencil lead, paper, and blending tools.

While the works discussed above are concerned with the low-level interaction of pigment with paper or canvas, other authors aid a user in the creation of an art work, or automate the artistic process. Haerberli [8] built a paint system that re-samples a digital image based on a brush. Wong [28] built a system for charcoal drawing that prompts the user for input at critical stages of the artistic process. Gooch et al. [7] automatically generated technical illustrations from polygonal models of CAD parts. Meier [15] produced painterly animations using a particle system. Litwinowicz [14] produced impressionist-style video by re-sampling a digital

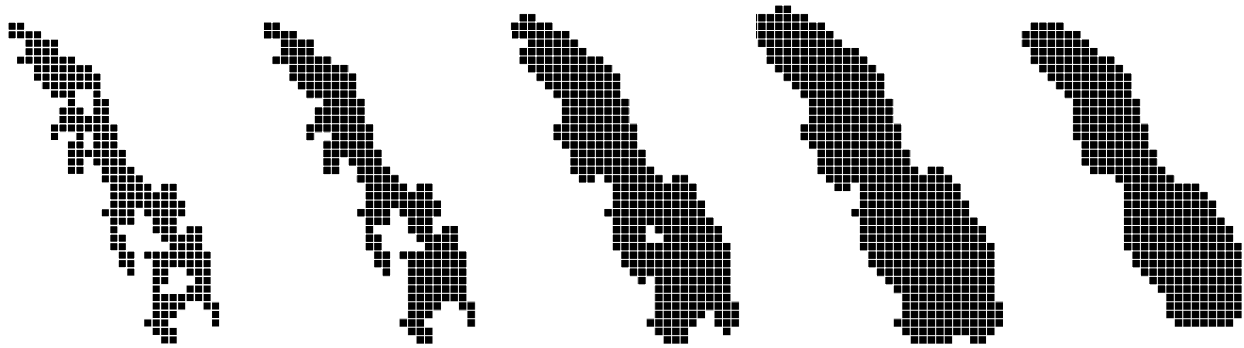


Figure 2: From left to right: An example of a segmented region. The region after the hole filling algorithm has been run. The region after being opened. The region after being opened again. The region after having been closed.

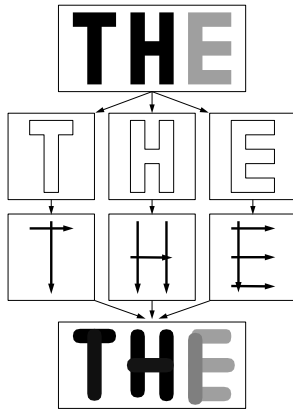


Figure 3: First an image is segmented using flood filling. Next each segment is independently decomposed into brush stroke paths. Finally brush strokes are rendered to a raster image.

image and tracking optical flow. Hertzmann [11] refined Haeberli’s technique by using progressively smaller brushes to automatically create a hand-painted effect. Shiraishi et al. [21] use image moments to create digital paintings automatically.

The algorithm described in this paper should be grouped with the latter set of works that simulate the high-level results of the artistic process. Our technique results in a resolution-independent list of brush strokes which can be rendered into raster images using any brush stroke rendering method.

### 3 Algorithm

Our system takes as input a digital image which is first segmented using flood filling (Sec 4). These segments are used to compute brush stroke paths. Using image processing algorithms, the boundaries of each segmented region are smoothed and any holes in the region are filled. The system next finds a discrete approximation to the central axis of each segment called the ridge set (Sec 5). Elements of the ridge set are pieced together into tokens (Sec 6). These tokens can, at the user’s discretion, be spatially sorted into ordered lists. In the final image this second sorting has the effect of painting a region with a single large stroke instead of many small strokes. Finally the brush paths are rendered as brush strokes (Sec 7). Figure 3 shows a diagram of our algorithm.

## 4 Segmentation and Smoothing

A technique sometimes used by artists is to first produce tonal sketches of the scene being painted [22]. These sketches are in effect low resolution gray scale images of the final painting that are used as a reference for form and lighting. Guided by this observation, we employ an intensity-based method of segmenting images.

An image is segmented by selecting an unvisited pixel, and searching outward for nearby unvisited pixels with similar intensities. “Similar intensity” is defined by the number of segmentation levels, and is based on a perceptual metric [9]. Pixels are marked as visited, and a new unvisited pixel is chosen. This is repeated until the entire image is quantized into independent segments.

Segments of similar intensity (such as the letters *T* and *H* in Figure 3) are not connected. This was useful in highly complex regions (such as the forest in Figure 4) because we were able to use the higher-level merging operations to chose stroke size rather than the intensity operations. We experimented with a number of segmentation operations, and found that this simple one was the most flexible. However, given the importance of segmentation on the final result, we think that more sophisticated segmentation strategies might prove beneficial.

### 4.1 Hole Filling

The segments produced in the previous step often have small holes due to shadows or highlights in the image. We use a standard hole-filling technique to remove these. Segmented regions are stored as boolean arrays with *true* indicating membership in the region. Each *false* pixel is queried to find how many *true* neighbors it has. Pixels with more than five *true* neighbors are changed to *true*. If a pixel has less than five neighbors, but is enclosed by an all *true* region, then the pixel is also set to *true*.

### 4.2 Morphological Operations

Opening and closing operations are used to smooth the boundary and remove noise. The Open operation changes every pixel from *false* to *true* if any of its neighbors are *true*. The Close operation changes every pixel from *true* to *false* if any of its neighbors are *false*. In practice we have found that two Open operations followed by a Close operation produced good results. The entire smoothing sequence is illustrated in Figure 2. Open and Close operations may also be applied to the approximate medial axis (described in the next section) with good results.

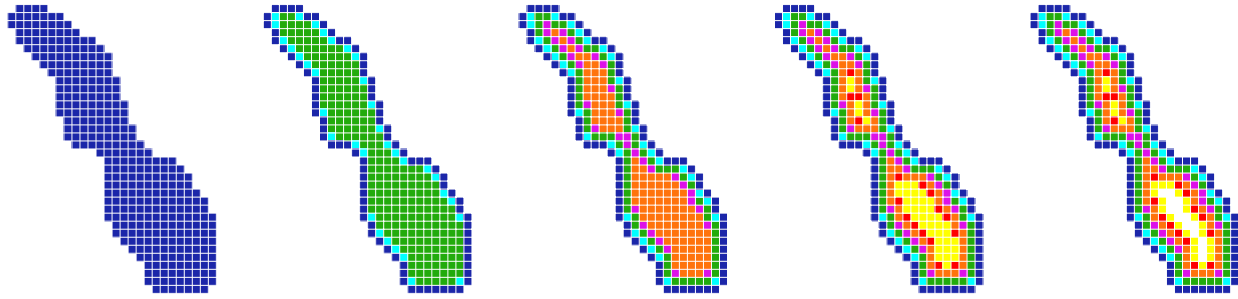


Figure 5: An example of a distance transform on a region from left to right. First each pixel in the region is initialized to 1 if it is in the segmented region, and to 0 if it is not. Next multiple passes are made over the region. At each pass, a pixel value is incremented if all non-zero neighbors have values less than or equal to the pixel’s current value. This example shows the increasing value of the pixels by changing the pixel color to a lighter gray.



Figure 4: An example of varying the number of gray levels in image segmentation. Top: the segmented image using 72 gray levels. Bottom: the segmented image using 48 gray levels. Note that the clouds have faded into the sky in the 48 gray level image.

## 5 Ridge Set Extraction

The medial axis of each segmented region is computed and used as a basis for the brush stroke rendering algorithm. The medial axis of a region is essentially the “skeleton” of an object. The medial axis transform yields scale and rotation invariant measures for a segment, which is a big advantage over other systems which rely upon grids. The medial axis was first presented by Blum [2], and has been shown to be useful in approximating 2D [13] and 3D objects [12]. The medial axis has also been shown to be a good approximation of the way the human visual system perceives shape [3].

While the medial axis is a continuous representation, there are several types of algorithms for computing the medial axis in image space, including thinning algorithms and distance transforms. Distance transform algorithms are not as sensitive to boundary noise and produce width information, but tend to produce double lines and don’t preserve connectedness [13]. Thinning algorithms, such as Rosenfeld’s parallel algorithm [18], preserve the connectedness and produce smooth medial axis lines. However these algorithms are sensitive to boundary noise, which will result in undesirable spurs along the medial axis. Another drawback to thinning algorithms is that they do not produce information about the distance to the boundary, which we need to estimate brush stroke width.

The positive aspects of both techniques are combined in our system to form a hybrid method. We first apply the distance transform to extract a discrete approximation of the medial axis called the ridge set. We then thin the ridge set to remove spurs (caused by boundary noise) and double lines (caused when the medial axis falls between pixels). This combination of techniques results in a ridge set with distance information, and reduced sensitivity to noise along the boundary.

### 5.1 Distance Transform

For each pixel in the region, we compute the shortest distance to the boundary [13]. On the first pass the distance transform algorithm assigns a value of one to each pixel in the region. Subsequent passes approximate a Euclidean distance transform by finding the smallest non-zero neighbor of the current pixel. If this pixel value is larger than the value of current pixel, it is incremented by 1 ( $\sqrt{2}$  if it is a diagonal neighbor). The algorithm proceeds until no values are changed during a pass. This process is shown in Figure 5. The number of passes is proportional to the radius of the largest circle that touches both boundaries.

### 5.2 Approximate Medial Axis Extraction

The next step is to extract the medial axis from the distance-transformed region. A discrete approximation to the medial axis is the ridge set, which is the set of points that are further away from the boundary of the region than any surrounding points. A pixel is part of the ridge set if its value is greater than or equal to the value of all 8 surrounding pixels [13].

This conservative definition of the ridge set may not yield a connected set of lines, which necessitates some of the later grouping algorithms. However, we found that using a less conservative test resulted in noisy line segments and nervous, uncontrolled brush strokes. This approximation avoids the problems of spurs associated with distance transforms, but produces numerous double lines.

To avoid these discretization problems, we are currently exploring a Voronoi diagram method which produces a continuous medial axis. However, the amount of computation required is usually larger than for the discrete method.

### 5.3 Thinning the Approximate Medial Axis

To address the problem of double lines in the distance transform, we use Rosenfeld’s parallel thinning algorithm [18]. This algorithm removes “redundant” pixels from a binary image by testing small neighborhoods of pixels. Each 8-pixel neighborhood is tested for redundant pixels. We developed a fast, unique test for these pixel neighborhoods; the details are discussed in the Appendix.

The thinning algorithm eliminates double-lines and other noise from the ridge set. The algorithm typically requires two to three passes over the ridge set. Another advantage of this thinning algorithm is that points in the ridge set are guaranteed to have at most three neighbors.

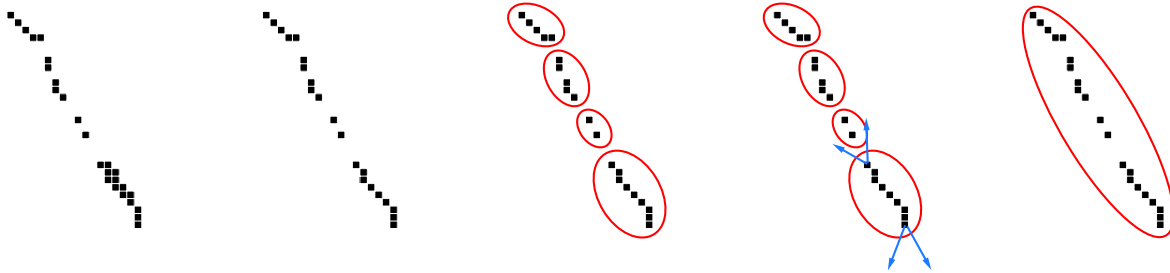


Figure 6: An example of ridge set extraction, thinning and grouping from left to right. First the ridge set is extracted from the distance transformed image. Second our thinning algorithm is applied. Third the resulting ridge set is grouped into tokens. Forth the tokens are merged into a stroke. The fifth image shows a set of tokens ready to be rendered

## 6 Ridge Set Tokenizing and Grouping

The combination of the distance transform and thinning algorithm yields a set of approximate medial axis points with associated width values. We next group spatially coherent points into tokens, as shown in Figure 6. A token is a higher order primitive which consists of 10 pixels. These tokens can then be grouped into strokes, and finally strokes from different segmentation regions may be grouped together. By operating on these higher order primitives rather than on pixels, we reduce noise and smooth the strokes.

We explored two methods for grouping tokens which differ in complexity, speed, and rendering techniques. These methods are compared in Secs 6.2 and 6.3.

### 6.1 Forming Tokens

The first step in tokenizing the ridge set is to classify pixels based on how many neighbors they have. Pixels are classified as follows:

- orphan** - no neighbors
- seed** - one neighbor
- line** - two neighbors
- branch** - three neighbors

Additional cases are not needed because the thinning algorithm guarantees at most 3 neighbors. During classification, queues for each type of point are created.

The tokens are grouped by performing a greedy search starting at seed points. Token objects are initialized as a single seed pixel. If the nearest neighbor to this point is also a seed, we start a new token. If the nearest neighbor point is a line point, we add the point to the token object and find the neighbor of the line point. If the nearest neighbor point is a branch point, we add the point to the token object, reclassify the point as a line point, and start a new token. Once the ridge set is grouped into tokens as in Figure 6, the tokens can be grouped into strokes.

In order to generate the color of a token, the color of each ridge point is generated by sampling the original image. A color value for the ridge point is calculated using the color ratios suggested by Schlick [20]. The color value for the token is then computed by taking a weighted average of all of the ridge points in the token.

### 6.2 Grouping Tokens via Moments

The first method we explored for grouping tokens into strokes was to compute the image moment of the token using the width values as

weights. The first moments yield the center of mass for the token which is used as the position. The second moments allow us to construct a major and minor axis for the token which are used as the length and width of the token. We were inspired by [21].

Using this moment information, we construct a dense graph of possible merges, then reduce this graph using a variant of Prim’s minimum spanning tree algorithm [5]. The graph is constructed by connecting every pair of tokens that are within a distance tolerance by an edge in the graph. A cost for each edge is computed by summing the differences of the tokens’ position, orientation, and color. For example, tokens that are at right angles incur a high edge cost, while tokens that are aligned have a low edge cost. These edges are loaded into a priority queue, and one by one the lowest cost edge is removed from the queue. If this candidate merge is feasible, then the tokens are merged. A merge is feasible if the tokens haven’t already been merged with other tokens. This usually means that the tokens are independent, or are at the ends of strokes. This process is repeated by until all the tokens are merged into a single stroke, or until all possible combinations of token merges have been attempted.

The merging process generates a set of strokes which cover the original set of tokens. Each token in the stroke has a width given by the minor axis of the moment of the token. The main drawback of this technique is computation time. The technique is  $O(N^2)$  on the number of tokens in the image and a large amount of computation is performed for each token. However, since it is a global method it tends to produce “optimal” strokes.

### 6.3 Grouping Tokens via Search Cones

We also explored a second method for grouping tokens which involves a greedy search in a conical region extending from the token. For each token, search cones are created along the major axis of the token, extending out a small distance. Then the cones of every token are tested to see if they intersect the cone of any other token. Tokens with intersecting cones are merged into strokes and the process is repeated until no further merges are possible. Unmerged tokens are made into single token strokes. Next, the algorithm attempts to merge the orphan tokens into the existing strokes by testing their positions verses the search cones.

The major advantages of this method over the moment method are speed, the cone intersections can be hard coded, and merging generally takes less than  $O(\log(N))$  passes over the data were  $N$  is the number of tokens. In addition, in order to render this type of stroke the ridge set points can be used directly without the overhead of computing B-spline curves. However, since this is a local method it may self-intersect and lack smoothness.



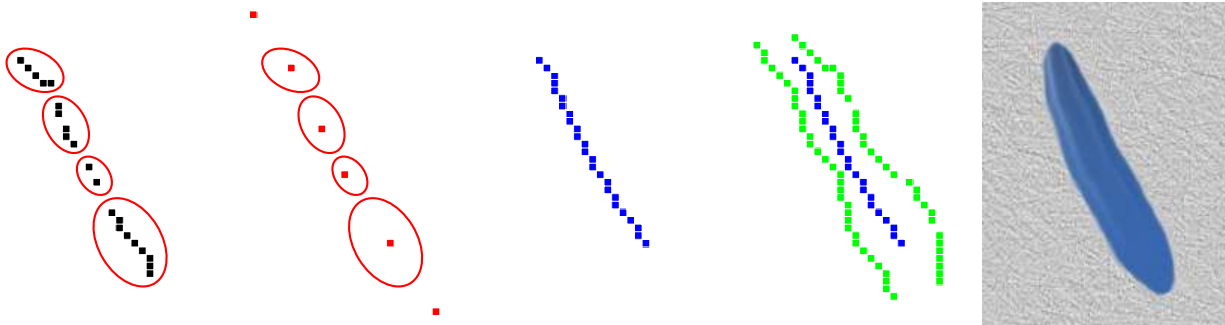


Figure 7: An example of our method for drawing strokes based on moment tokens. First, points are grouped into tokens and the moment of the group is taken. Second, points are replaced by the moment centroid and additional points are added to the beginning and end of the token list. Third, the points are used as the control polygon of a B-spline curve. Forth, offset curves are computed based upon the width values. Last, the stroke is rendered.

## 7 Rendering Images

Brush stroke rendering depends on the method of token grouping used in the previous phase of the algorithm. Modified versions of Strassman [24] and Pham’s [17] algorithms are used to render brush strokes. Strassman and Pham modeled sumi-e brushes which taper on from a point and taper off to a point during a brush stroke. We choose to model a Filbert brush used in oil painting. Filbert brushes are good all-purpose brushes combining some of the best features of flat and round brushes [22]. To model a Filbert brush, the taper-on is constrained to a circular curve and the taper-off constrained to a parabolic curve. Examples of this type of simulated brush stroke are shown in Figure 15.

### 7.1 Stroke Representation

Strokes made up of tokens that are grouped using the moment method are rendered using the positions of the moments as the control points of a B-spline curve. This list of control points is called the control polygon. Since B-spline interpolation has the side effect of shortening the stroke, we add extra points on the beginning and the end to compensate (see Figure 7). In addition to the control polygon, we compute a scalar spline curve that blends the width values. Using this width spline and the control polygon, we render the strokes by drawing parallel lines in the direction of the brush stroke.

Strokes that are grouped using the search cone method are rendered using a simpler method. Normals are calculated using the finite differences of the token centers, and the widths are sampled from the nearest token. From these values a quadrilateral is generated, and filled using lines perpendicular to the normal.

This method has the advantages of speed and a great deal less computational and coding complexity than the B-spline method. However, due to the absence of blending, this method can create visible artifacts when used with alpha blending. The normal directions calculated for each of the stroke points can intersect, causing what Strassmann [24] called the “bow tie” effect. This effect is demonstrated in Figure 9. When a low alpha values are used, causing the brush stroke to appear opaque, and the brush stroke contains these self intersections, these areas of the stroke appear darker. In practice this effect is generally not noticeable with alpha values higher than 0.75.

### 7.2 Grouping Strokes

In addition to grouping tokens and strokes inside a single segmented region, strokes and tokens from different regions can be merged. An

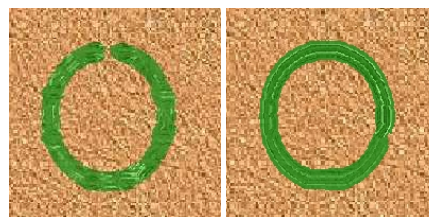


Figure 8: A region painted without a grouping algorithm. (left image: 62 strokes), and with (right image: 1 stroke)

example is shown in Figure 8. In theory, this should smooth strokes and generate a more pleasing flow. In reality, the effect upon images varies, and may not be suitable in every case. Stroke merging can use either the moment method or the search cone method. The moment method incurs a large memory overhead due to the fact that all of the tokens and strokes from all regions need to be saved and checked. In practice this slows the system down by between one and two orders of magnitude depending on the image size and the available memory.

## 8 Underpainting and Brush Effects

Underpainting is simulated by allowing the user to render strokes on top of another image. Meyer [15], Hertzmann [11], and Shiraishi et al. [21] discuss underpainting in their work. Meyer rendered brush strokes on an a background image. Hertzmann and Shiraishi blur the source image and render strokes on the blurred image.

Our system allows the user to import separate source images and underpainting images. In this way, strokes can be rendered onto a background image or onto blurred images. In addition the underpainting can be used for artistic effect as in Figure 13. The output of the system could also be used as an underpainting allowing a painting to be built up in layers.

Painting effects such as brush artifacts, paint mixing between layers, and stroke connection are also possible in the system. Alpha blending is used to simulate paints of various opacity. Paints with a high opacity will show the underlying substrate while paints with a low opacity will block the view of the substrate. The alpha parameter controls the percentage of blending between the underpainting and the brush strokes.

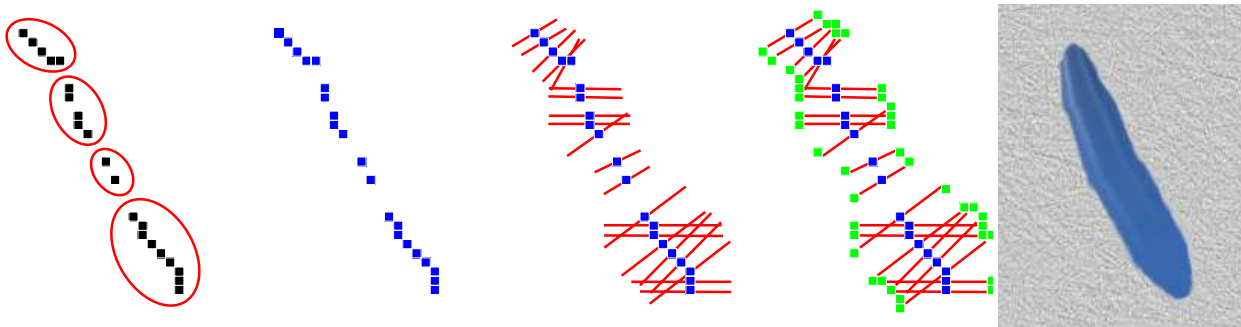


Figure 9: An example of our method for drawing strokes based on line lists. First, points are grouped into tokens. Second, tokens are grouped into a list of points. Third, for every point a normal line is found. Forth, based on the normal directions and the width at each point edge points for the stroke are computed. Last, a brush stroke is rendered.

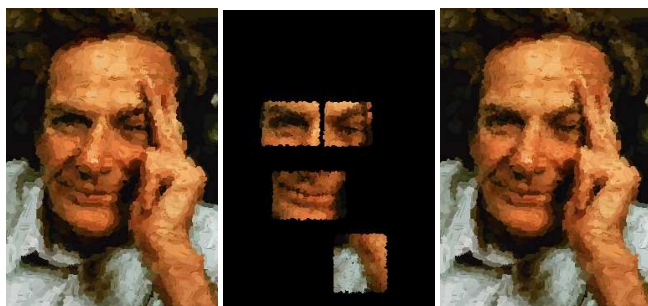


Figure 10: An example of user-directed enhancement. The Feynman portrait is deemed by the user to lack detail in regions surrounding the eyes, mouth, and hand. The user selects these regions, and raises the segmentation level. New higher frequency strokes are drawn over the original strokes, hopefully improving the result.

## 8.1 User-Directed Enhancement

Human artists often apply brush strokes in a manner which communicates the underlying three dimensional structure of the subject. Because we have no three dimensional information about the source image we implemented two heuristic techniques. The first is to start brush strokes at the widest end of the stroke. The second method allows the user to select areas of interest in the image and resegment these areas with a higher number of gray levels. As discussed in Section 4, a single set of segmentation levels is chosen for the entire image. Increasing the number of gray levels in the segmentation increases the number of strokes, which changes the impression of a painting. This difference has a strong effect on the painted image as seen in Figure 14.

The user can select areas of interest in the image and these areas are repainted with a higher number of strokes. This allows the user to direct the placement of high frequency information in the image, and in many cases improves the visual appearance of the painting. This is similar in spirit to the method of Hertzmann [10]. An example of this process is shown in Figure 10.

## 9 Extension: Depth Information

While working with this system, we have noticed that certain input images generated nice paintings while others do not. In particular, landscape scenes tend to work very well, while closeups (such as portraits) tend not to turn out as well, and may require manual resegmentation. We believe that there are a number of reasons for

this, the primary one being painting is an inherently 3-dimensional process. Artists have spent hundreds of years refining 3D techniques, beginning in the Renaissance [1]. In addition, there have been numerous computer 3D painting techniques [2]. We applied some of these techniques to our system as a first step in incorporating 3D information into our 2D painting algorithm.

In Section 9.1, we talk about different techniques artists have developed, and in Section 9.2 we talk about how we applied these techniques to our painting system.

### 9.1 Artistic Techniques for Creating Space

Artists create space and distance using techniques such as perspective, detail variation, color saturation, atmospheric perspective, and warm/cool fades. The perspective effect and the detail variation are in some sense already present in images, from the mechanisms inherent in photography. We were most interested in applying the warm-to-cool fade. The warm colors - red, orange, yellow - "psychologically suggest emotion, energy and warmth while optically moving the subject to the foreground." [19] The cool colors - green, blue, violet "appear to recede." [19]

### 9.2 Applying these Ideas

There are a number of ways to generate depth information, including depth-from-stereo, depth-from-shading, etc. [25], as well as synthetic images, where the depth is explicitly represented in a depth buffer.

Any of these techniques will work for our system. Synthetic images have an advantage in that they are easy to obtain and have a regular, noise-free depth map. Depth-from-stereo produce somewhat noisy depth maps (based on image texture), can be hard to obtain, and often require some manual input to identify corresponding image features. However, these images are usually more visually interesting than synthetic images.

Once the depth map has been calculated, it is fed into the painting system along with the input image. The depth is used as another information channel to the segmentation process. Objects are first differentiated using the depth, and these objects are further decomposed using intensity variation. This technique was chosen because depth tends to be quite good at resolving object-object interactions, but poor at choosing how to lay strokes across a surface. Likewise, intensity can often fail to correctly identify separate objects, but does well at placing strokes across a surface.

The depth is used to vary the levels of segmentation in the image by segmenting at a low level for distant objects and at a high level for close objects. This tends to increase the detail in close objects while decreasing detail in distant objects.



Figure 11: An example of using depth segmentation. From left to right: the original image, the depth image, the painting without using the depth information, and the painting using depth information. No underpainting was used (for comparison)

The algorithm then uses these segments in the same way as before, and generates a set of strokes. These strokes maintain properties such as intensity and depth. The depth is then used to modulate the color of the stroke, using the warm-to-cool fade mentioned above. In the future, we intend to also implement the color saturation and atmospheric effects. These operations are shown in Figures 11 and 16.

### 9.3 Depth Extension Analysis

It is clear that using depth information can increase the quality of the painting. We believe that this is because painting is an inherently 3D process, and only using image processing techniques in 2D hinders the process. However, there are several issues still to be considered.

The depth information is often noisy and incomplete, particularly if the depth map is obtained using stereo cameras or other depth-from-X techniques. This confuses the segmentation process, resulting in a noisy segmentation (and ultimately, a noisy painting). This could be handled by assigning weights to the intensity information and depth information, allowing the user (or the algorithm) to compensate for noisy or incomplete data. The technique is not applicable to portrait painting, as the depth gradient is quite small across a face. There may be other artistic techniques for portrait painting that would be more amenable to computer implementation.

We intend to explore: Are there other techniques that could be applied to computer algorithms? Are the applications of these techniques used in this system correct, or do they bias the painting unnecessarily? Are there better ways of providing tools for users to experiment? Perhaps users want more control over the process of painting, instead of less control?

## 10 Conclusion and Future Work

We think productive future work would include improvements to every stage of the algorithm. Images which require sophisticated segmentation, and images where viewers are sensitive to the features of the image, such as detailed portraits, can cause the method to fail. Better segmentation, such as that given by anisotropic diffusion [26], may yield immediate improvements in linking brush strokes to salient features of the image. The computation of medial axes might be less sensitive to noise if a continuous medial axis algorithm based on Voronoi partitions were used. This may also simplify the job of token-merging in our algorithm by reducing input noise. A sophisticated ordering of brush strokes, such as optimizing order based on edge correlation with the original image might improve the painting, but would come with huge cost in computation

and memory usage. A more physically-based paint-mixing would give a look more reminiscent of oil painting.

Our system might also benefit from a user-assisted stage at the end to improve brush stroke ordering. An estimate of foveal attractors in the image could allow brush stroke size to be varied with probable viewer interest. Most challenging, our method could probably be extended to animated sequences, using time-continuous brush-stroke maps to ensure continuity. However, it is not clear what such animated sequences would look like, or to what extent they are useful. The most exciting future effort is to create an actual stroke-based hard copy using robotics or other technology.

## 11 Acknowledgments

We would like to thank Amy Gooch, Kavita Dave, Bill Martin, Mike Stark, Samir Naik, the University of Utah Graphics Group and the University of North Carolina Graphics Group for their help in this work. This work was carried out under NSF grants NSF/STC for computer graphics EIA 8920219, NSF/ACR, NSF/MRI and by the DOE AVTC/VIEWS.

## Appendix: Thinning Algorithm

Rosenfeld’s thinning algorithm tests each pixel neighborhood for redundant pixels. Since this test is performed at each pixel in the image, it is important that it be fast. We have developed an original technique for determining whether a pixel is redundant.

In this Appendix, we describe the test that is performed at each pixel. The input is the pixel’s 8-neighborhood, and the output is a boolean telling whether this pixel is redundant. The idea of this test is to construct a graph of all of the paths through this neighborhood, then test whether removing the center pixel breaks any of these paths. If it does not, then the center pixel represents a redundant path. If it does, then the center pixel must remain (this is called *8-simple*).

### Observations

The first step is to construct a graph  $G(V, E)$  that connects every pixel, except for the center pixel, to its adjacent pixels. This is illustrated in Figure 12.

This graph  $G$  represents the paths through this neighborhood. The test for 8-simplicity just becomes a test for the connectedness of  $G$ . We can use Euler’s Theorem for connected planar graphs, which states that  $v + r - 2 = e$ , where  $v$  denotes vertices,  $r$  denotes regions of plane,  $e$  denotes edges. Rearranging the terms yields two conditions for 8-simplicity in a pixel neighborhood: 1) there can be no isolated pixels; 2)  $v - 1 \leq e$ .

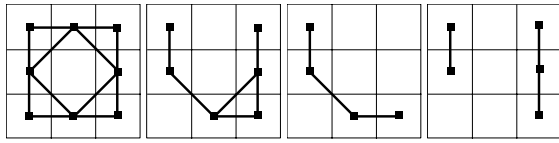


Figure 12: From left to right: The graph representation of a full neighborhood. An 8-simple neighborhood. Another 8-simple neighborhood. A non-8-simple neighborhood.

## Implementation

Let the edges of  $G$  be  $E_i$ , and a graph representation of a full neighborhood be  $N$ . Then the algorithm is:

```

for each  $i \in G$  {
  //Test for isolated pixels
  if (  $E_i \cap N = \phi$  ) return not_simple;
  // Else add to the total edges
  else edges += degree(  $E_i \cap N$  );
}
// Euler's Theorem.
if ( edges  $\geq v - 1$  ) return simple;
else return not_simple

```

## Notes

We encoded the  $E_i$  and  $N$  in binary, resulting in a fast test. The only storage requirements are the eight sets  $E_i$ , which can be stored as eight integers. Most previous thinning algorithms in the computer graphics literature enumerate and store every case, resulting in a large overhead.

## References

- [1] BERMAN, D. F., BARTELL, J. T., AND SALESIN, D. H. Multiresolution painting and compositing. *Proceedings of SIGGRAPH 94* (1994), 85–90.
- [2] BLUM, H. A transformation for extracting new descriptions of shape. *Models for the Perception of Speech and Visual Form* (1967), 362–380.
- [3] BURBECK, C. A., AND PIZER, S. M. Object representation by cores: Identifying and representing primitive spatial regions. *Vision Research* 35, 13 (1995), 1917–1930.
- [4] COCKSHOTT, T. *Wet and Sticky: A Novel Model for Computer-Based Painting*. PhD thesis, University of Glasgow, 1991.
- [5] CORMEN, T., LEISERSON, C., AND RIVEST, R. *Introduction to Algorithms*. MIT Press, 1990.
- [6] CURTIS, C. J., ANDERSON, S. E., SEIMS, J. E., FLEISCHER, K. W., AND SALESIN, D. H. Computer-generated watercolor. *Proceedings of SIGGRAPH 97* (August 1997), pages 421–430.
- [7] GOOCH, B., SLOAN, P.-P. J., GOOCH, A., SHIRLEY, P., AND RIESENFELD, R. Interactive technical illustration. *1999 ACM Symposium on Interactive 3D Graphics* (April 1999), 31–38.
- [8] HAEBERLI, P. E. Paint by numbers: Abstract image representations. *Proceedings of SIGGRAPH 90* 24, 4 (August 1990), 207–214.
- [9] HEARN, D., AND BAKER, M. P. *Computer Graphics*. Prentice-Hall, 1986.
- [10] HERTZMANN, A. Paint by relaxation. In *Computer Graphics International 2001* (July 2001), pp. 47–54. ISBN 0-7695-1007-8.
- [11] HERTZMANN, A. Painterly rendering with curved brush strokes of multiple sizes. *Proceedings of SIGGRAPH 98* (July 1998), 453–460.
- [12] HUBBARD, P. M. Approximating polyhedra with spheres for time-critical collision detection. *ACM Transactions on Graphics* 15, 3 (July 1996), 179–210.
- [13] JAIN, R., KASTURI, R., AND SCHUNCK, B. *Machine Vision*. McGraw-Hill, 1995.
- [14] LITWINOWICZ, P. Processing images and video for an impressionist effect. *Proceedings of SIGGRAPH 97* (August 1997), 407–414.
- [15] MEIER, B. J. Painterly rendering for animation. *Proceedings of SIGGRAPH 96* (August 1996), 477–484.
- [16] PERLIN, K., AND VELHO, L. Live paint: Painting with procedural multiscale textures. *Proceedings of SIGGRAPH 95* (August 1995), 153–160.
- [17] PHAM, B. Expressive brush strokes. *Computer Vision, Graphics, and Image Processing. Graphical Models and Image Processing* 53, 1 (Jan. 1991), 1–6.
- [18] ROSENFELD, A. A characterization of parallel thinning algorithms. *InfoControl* 29 (November 1975), 286–291.
- [19] SASAKI, H. Color psychology. <http://www.shibuya.com/garden/colorpsycho.html> (April 1991).
- [20] SCHLICK, C. Quantization techniques for visualization of high dynamic range pictures. *Proceedings of the 5th Eurographics Workshop* (June 1994), 7–20.
- [21] SHIRAISHI, M., AND YAMAGUCHI, Y. An algorithm for automatic painterly rendering based on local source image approximation. *NPAR 2000 : First International Symposium on Non Photorealistic Animation and Rendering* (June 2000), 53–58.
- [22] SMITH, A. R. Varieties of digital painting. Tech. rep., Microsoft Research, August 1995.
- [23] SOUSA, M. C., AND BUCHANAN, J. W. Computer-generated graphite pencil rendering of 3d polygonal models. *Computer Graphics Forum* 18, 3 (September 1999), 195–208.
- [24] STRASSMANN, S. Hairy brushes. *Siggraph* 20, 4 (Aug. 1986), 225–232.
- [25] TRUCCO, E., AND VERRI, A. *Introductory Techniques for 3-D Computer Vision*. Prentice-Hall, 1998.
- [26] TUMBLIN, J., AND TURK, G. LCIS: a boundary hierarchy for detail-preserving contrast reduction. *Proceedings of SIGGRAPH 99* (August 1999), 83–90. ISBN 0-20148-560-5. Held in Los Angeles, California.
- [27] WILLIAMS, L. 3D paint. *1990 Symposium on Interactive 3D Graphics* (1990), 225–233.
- [28] WONG, E. Artistic rendering of portrait photographs. Master's thesis, Cornell University, 1999.





Figure 13: Underpainting is a method used by artists to block in basic forms and values in a painting. We simulate underpainting by allowing the user to render strokes on top of another image. This example shows a source image. Next a painting made from this image using the source image as an underpainting. The third image is an underpainting made by changing the color gamut of the original image and then blurring the image. The final painting was made by painting strokes, using the first image as a source, onto the modified underpainting. This technique can be expanded to create images with multiple painted layers.

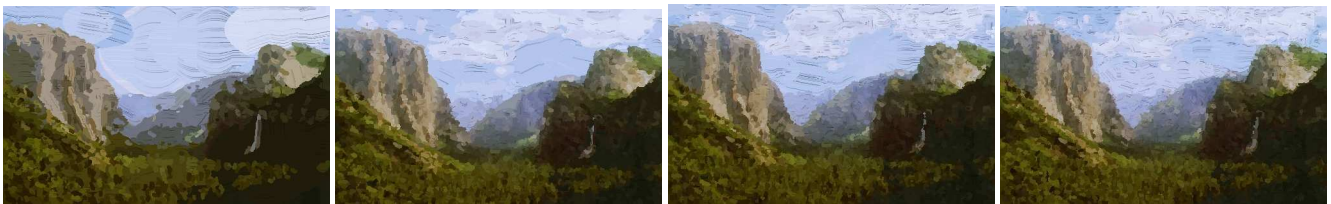


Figure 14: An example of varying the number of gray levels in the segmentation and the resulting paintings. From top to bottom the images were segmented using; 12, 48, 72, and 150 gray levels.

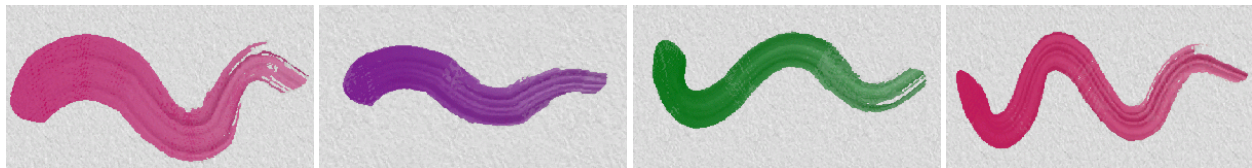


Figure 15: Digitally simulated brush strokes. These images demonstrate the range of brush effects.



Figure 16: An example of using depth segmentation. From left to right: the original image, the depth image, the painting without using the depth information, and the painting using depth information. No underpainting was used (for comparison)